Journal of Molecular Neuroscience (2018) 64:397–409
https://doi.org/10.1007/s12031-018-1036-z

Quantitative Comparison of Primary Cilia Marker Expression and Length in the Mouse Brain

Éva Sipos[1] · Sámuel Komoly[1] · Péter Ács[1]

Received: 22 December 2017 / Accepted: 31 January 2018 / Published online: 20 February 2018

Abstract

Primary cilia are small, special cellular organelles that provide important sensory and signaling functions during the development of mammalian organs and coordination of postnatal cellular processes. Dysfunction of primary cilia are thought to be the main cause of ciliopathies, a group of genetic disorders characterized by overlapping developmental defects and prominent neurodevelopmental features. Although, disrupted cilia-linked signaling pathways have been implicated in the regulation of numerous neuronal functions, the precise role of primary cilia in the brain are still unknown. Importantly, studies of recent years have highlighted that different functions of primary cilia are reflected by their diverse morphology and unique signaling components localized in the ciliary membrane. In the present study, we conducted a comparative analysis of the expression pattern, distribution and length of adenylyl cyclase 3, somatostatin receptor 3, and ADP-ribosylation factor-like protein 13B expressing primary cilia in the mouse brain. We show that cilia of neurons and astrocytes display a well characterized distribution and ciliary marker arrangements. Moreover, quantitative comparison of their length, density and occurrence rate revealed that primary cilia exhibit region-specific alternations. In summary, our study provides a comprehensive overview of the cellular organization and morphological traits of primary cilia in regions of the physiological adult mouse brain.

Keywords Primary cilia marker expression · Length · Distribution · CNS

Abbreviations

$5HT_6$	Somatostatin receptor 6
AC3	Adenylyl cylase type 3
ARC	Arcuate nucleus
Arl13b	ADP-ribosylation factor –like protein 13 B
AsPC	Astrocytic primary cilia
BBS	Bardet-Biedl syndrome
CNS	Central nervous system
D1r	Dopamine receptor subtype 1
DM	Dorsomedial nucleus
GFAP	Glial fibrillary acidic protein
GPCR	G protein-coupled receptor
Kiss1r	Kisspeptin receptor 1
Mch1r	Melanin-concentrating hormone receptor subtype 1
NeuN	Neuronal specific nuclear protein
NPC	Neuronal primary cilia
NPY2r	Neuropeptide Y 2 receptor
NPY5r	Neuropeptide Y 5 receptor
PVN	Paraventricular nucleus
SCN	Suprachiasmatic nucleus
Sstr3	Somatostatin receptor subtype 3
VM	Ventromedial nucleus

Electronic supplementary material The online version of this article (https://doi.org/10.1007/s12031-018-1036-z) contains supplementary material, which is available to authorized users.

✉ Éva Sipos
eve.sipos@gmail.com

[1] Department of Neurology, Faculty of Medicine, University of Pécs, Rét utca 2, Pécs 7623, Hungary

Introduction

Primary cilia are solitaire, non-motile organelles on the surface of most mammalian cells types. Based on their distinctive position on the cells, primary cilia have been designated to serve as cellular antennas that coordinate numerous developmental and physiological signaling pathways (Gerdes et al. 2009; Marshall and Nonaka 2006; Singla and Reiter 2006). Cellular loss of primary cilia or impaired function of ciliary proteins results in abnormal signal transduction towards the cells, which is thought to underlie a wide range of human genetic disorders, collectively

termed ciliopathies (Badano et al. 2006). Some human ciliopathies such as Bardet-Biedl Syndrome, Joubert Syndrome, Alström Syndrome, or Meckel-Grüber Syndrome comprise severe central nervous system (CNS) involvement including cognitive deficits, mental retardation, and brain malformations (Barker et al. 2014; Forsythe and Beales 2013; Marshall et al. 2011; Parisi 2009; Sattar and Gleeson 2011). Although dysfunctional primary cilia are known to cause a broad spectrum of neurological disorders, their precise functions in the brain are still vaguely known.

In the CNS, primary cilia on neurons are known to be enriched for specific G protein-coupled receptors (GPCRs) including somatostatin 3 receptor (Sstr3) (Handel et al. 1999), melanin-concentrating hormone receptor subtype 1 (Mch1r) (Berbari et al. 2008a; Berbari et al. 2008b), serotonin receptor 6 ($5HT_6$) (Brailov et al. 2000; Hamon et al. 1999), dopamine receptor 1 (D1r) (Domire et al. 2011), kisspeptin receptor 1 (Kiss1r) (Koemeter-Cox et al. 2014), neuropeptide Y 2 and 5 receptor (NPY2r and NPY5r) (Loktev and Jackson 2013), as well as downstream signaling molecules such as type 3 adenylyl cyclase (AC3) (Bishop et al. 2007). Notably, ciliary expression of these signaling proteins are known to be restricted to different subsets of neurons in the brain.

Primary cilia have been implicated in the regulation of the hypothalamus, the main controlling center of feeding behavior. Many concise studies have highlighted that specific molecules concentrated in cilia of hypothalamic neurons—such as Mch1r, AC3 and Bardet-Biedl Syndrome proteins (BBS)—contribute to the complex signaling pathways coordinating appetite (Berbari et al. 2008a; Berbari et al. 2008b; Einstein et al. 2010; Pissios et al. 2006; Schou et al. 2015). In particular, genetic loss of ciliary structure or certain proteins have been shown to profoundly compromise signaling cascades and cause hyperphagia-induced obesity in mice under different experimental conditions (Davenport et al. 2007; Wang et al. 2009). Besides the hypothalamus, the hippocampus is also a region where disruption of neuronal primary cilia (NPC) have been proven to have a significant influence on neuronal connections and adversely affect learning, memory, as well as novel object recognition in mice (Einstein et al. 2010; Wang et al. 2011).

Possible functions of primary cilia are also reflected by changes in ciliary morphology and length. Adaptation of cilium length—such as elongation—has been proposed to fine-tune the signaling activity of the organelle in response to changes in extracellular environment (Dummer et al. 2016; Hilgendorf et al. 2016). Moreover, abnormal signaling indicated by either altered morphology or the loss of ability to adjust might be pathological hallmarks of NPC related diseases. Similarly to GPCRs, ADP-ribosylation factor-like protein 13B (Arl13b) also localizes to primary cilia and plays a direct role in the initiation, differentiation, and elongation of the organelle (Cevik et al. 2010; Kasahara et al. 2014; Larkins et al. 2011; Lu et al. 2015). Arl13b belongs to the Ras superfamily of small GTPases that has a dedicated role in wide range of different cellular processes (for review see: (D'Souza-Schorey and Chavrier 2006; Gillingham and Munro 2007). Cells lacking functional Arl13b exhibit significantly shortened and structurally altered cilia, whereas overexpression of Arl13b increases ciliary length on the cells (Caspary et al. 2007; Larkins et al. 2011; Lu et al. 2015). In line with this, studies have also reported that pharmacological activation, inhibition or genetic absence of other ciliary signaling components can also influence cilium length and morphology under different experimental conditions (Miyoshi et al. 2009; Miyoshi et al. 2014; Ou et al. 2009). Despite all of these observations, our knowledge about the precise roles of primary cilia in the CNS are still not fully understood. To further investigate the relationship between primary cilia and brain functions, we aimed to characterize the regional distribution and length of AC3, Sstr3, and Arl13b expressing primary cilia in the mouse brain.

In line with previous studies, we found that AC3 and Sstr3 localize to neuronal primary cilia, while Arl13b expression is strongly associated with primary cilia on astrocytes. Moreover, we report that neuronal and astrocytic primary cilia display regional alternations in length. Finally, we show that there is a distributional pattern and preference of primary ciliary marker expression in distinct areas of the brain.

Materials and Methods

Animals and Ethics Statement

For all experiments, 8-week-old male C57/Bl6 mice were used (Charles River Laboratories Magyarország Kft, Isaszeg, Hungary). Animals were housed in groups 3–4, kept in standard conditions at 24 °C (12-h light dark cycle) and were provided standard rodent chow and water ad libitum. Their general appearance as well as health status was observed daily and their weight was monitored three times a week until the day of experiment.

Animal experiments were conducted according to the European legislation on animal experimentation [Directives of the European Community (DIRECTIVE 2010/63/EU) and Hungarian regulations (40/2013, II.14)] in the laboratories of the University of Pécs.

The project was approved by local and national ethical boards and license was issued by government authorities (License No.:BA02/2000-44/2016 (KA-2068)).

Experimental Procedures

Tissue Preparation

For histological studies, mice were deeply anesthetized with 70 mg/kg I.P. sodium-pentobarbital (Euthasol) solution. After

that, mice were intracardially perfused with phosphate buffered saline (pH 7.2; PB) followed by 4% paraformaldehyde in 0.1 M phosphate buffer (PB). Brains were carefully dissected under microscopic control and were subjected to overnight postfixation in the same fixative at 4 °C. Then, brains were cryoprotected in 30% sucrose in PB overnight and coronally sectioned with a freezing microtome. For immunohistochemical studies, 30-μm-thick, free-floating sections were collected and stored in 1% sodium-azide solution at 4 °C for a maximum of 3–14 days until further processing. For immunofluorescence studies, 8-μm-thick brain sections were mounted onto gelatine-coated slides and kept at − 80 °C until used.

Immunohistochemistry

Free-floating brain sections were treated with 3% hydrogen peroxide in 0.1 M PB (pH 7.2), were rinsed in PB three times, and were permeabilized with 0.5% Tx100 in PB, 0.1% sodium-azide (NaN_3), and 30 mg/ml bovine serum albumin (BSA). Thereafter, sections were washed again three times and incubated with primary antibody diluted in Tx100/PB/NaN_3/BSA overnight at 4 °C. The following antibodies were used: rabbit polyclonal anti-adenylyl cylase subtype 3 (AC3) (1:1000, Santa Cruz, Cat.No.: sc-588), rabbit polyclonal anti-somatostatin receptor 3 (Sstr3) (1:2000, Thermo scientific, Cat.No.: PA3-207) and rabbit polyclonal anti-ADP rybosylation factor-like protein 13 B (Arl13b) (1:2000, Protein Tech, Cat.No.: 17711-1-AP). For visualization, appropriate anti-rabbit biotin-conjugated secondary antibody (1:1000) and avidin-biotin complex (1:500)(ABC, Vectastain kit, Vector Laboratories) was applied according to the manufacturer's manual. Following rinses in PB and once in 0.05 M Tris buffer (pH 8.2, TRIS), the reaction product was generated by 3'3'-diamimobenzidine-nickel-sulfate (DAB-nickel) solution. Tissue was mounted onto gelatine-coated slides and counterstained with 1% neutral red to detect neuronal cell bodies.

Slides were digitized with an automated whole slide scanner (Pannoramic 250 Flash II scanner, 3DHistech Ltd., Budapest, Hungary) equipped with a three-CCD (charge-coupled device) digital camera (CIS 3CCD, 2 megapixel, CIS Corporation, Tokyo, Japan). High-resolution images were captured by using Pannoramic Viewer software.

Immunofluorescent Studies

Immunofluorescent procedures were conducted as previously described (Saghy et al. 2016). Briefly, 8-μm-thick, gelatine-coated slides were brought to room temperature, rehydrated in 0.1 M phosphate buffered saline (pH 7.6; PBS) and heat-unmasked in 10 mM citrate buffer (pH 6.0). Sections were blocked in Power Block solution (Biogenex Life Sciences) and incubated overnight with primary antibodies diluted in 1% normal horse serum (Vector Laboratories). Primary cilia were labeled with the same antibodies applied in IHC, namely rabbit polyclonal anti-adenylyl cylase subtype 3 (AC3) (1:500, Santa Cruz), rabbit polyclonal anti-somatostatin receptor subtype 3 (Sstr3) (1:1000, Thermo Scientific), and rabbit polyclonal anti-ADP rybosylation factor-like protein 13 B (Arl13b) (1:1000, Protein Tech). For the detection of CNS cell types, rabbit polyclonal anti-RBFOX3/NeuN (NeuN) (1:200, Novus Biologicals) was applied to identify neurons, rabbit polyclonal anti-glial fibrillary acidic protein (GFAP) (1:500, Dako) to visualize astrocytes, mouse monoclonal anti-adenomatosus polyposis coli (APC) (1:500, Calbiochem) to detect mature oligodendrocytes, and rabbit polyclonal anti-ionized calcium binding adaptor molecule 1 (Iba-1)(1:500, Abcam) was used as a marker of microglia/macrophages (panmacrophage). For visualization of AC3, Sstr3, and Arl13b and for double immunofluorescence analysis, sections were incubated with appropriate Alexa fluor 594/488-conjugated secondary antibodies (Invitrogen) or with appropriate HRP-conjugated secondary antibodies (Biogenex) followed by signal amplification with Alexa labeled 594 or 488 tyramide (1:500, Tyramide Amplification kit, Invitrogen) according to the manufacturer's protocol. All sections were labeled with 4′6-diaminidino-2-phenylindol (DAPI) (Invitrogen) for visualizing cell nuclei.

Fluorescent images were taken with Axio Scope A1 fluorescent imaging system (Zeiss, Germany) attached to a Canon Powershot A620 digital camera and Isis software (Metasystem, Germany).

Quantification and Length Measurement of Primary Cilia

Assessment of primary cilia distribution and length were carried out in 19 different regions of the brain according to the mouse brain atlas of Paxinos and Franklin (Franklin and Paxinos 2008). Regions of interests were summarized in Supplementary Fig. 1 (Online Resource, Fig. 1). Sections were photographed at ×20, ×40, and ×60 magnification by using the Pannoramic Viewer or ISIS software. All raw images were processed and analyzed by using Fiji-ImageJ software. Quantification of primary cilia was achieved by counting the number of immunopositive structures on neurons and astrocytes in the different regions of the brain. The length of each primary cilia was determined for 150–200 co-labeled cells per region utilizing the double immunofluorescent labeled sections. To obtain accurate measurements, primary cilia length assessment involved only those cilia which aligned longitudinal in plane and sharpness was observed from base to the tip. Measurements were repeated three times for each ciliary marker per brain region and animal. All data from primary cilia measurements were collected, a mean value was generated and used for statistical analysis.

Statistical Analysis

Statistical analyses were made using GraphPad Prism Version 6 (GraphPad Software, San Diego, CA). The comparative distribution of ciliary markers was determined by the fraction of total analysis, in which all three ciliary markers co-labeled with NeuN or GFAP were separately counted and were divided by the total number of primary cilia calculated in each brain region.

The length of AC3-, Sstr3-, or Arl13b-positive primary cilia on neurons and astrocytes was also measured individually. After all measurements were collected, a mean value was separately generated for each marker in each investigated brain area. Then, comparison of cilia length was conducted, in which a marker's average length was statistically compared to the value of the other marker or markers present in each region, respectively (unless stated otherwise, shorter or longer terms are used in the following sections to refer to the statistical comparison of the length of labeled cilia on neurons and astrocytes within a brain region).

Statistical differences within distinct regions were tested with unpaired *t* tests or with one-way ANOVA followed by Tukey's multiple comparison post hoc test.

Differences were considered significant $P < 0.05$. Unless otherwise noted, all data represent ± SEM.

Results

Characterization of AC3, Sstr3, and Arl13b Expressing Primary Cilia of CNS Cell Types

To assess the distribution of ciliary markers in the mouse brain, we first analyzed the localization of AC3, Sstr3, and Arl13b positive primary cilia of different CNS cell types. Brain sections were co-immunolabeled with antibodies to the three ciliary markers and with NeuN for neurons, GFAP for astrocytes, APC for mature oligodendrocytes or Iba-1 for microglia/macrophages. In line with previous reports (Bishop et al. 2007; Handel et al. 1999), the majority of AC3 positive and all Sstr3-positive primary cilia were detected on the surface of NeuN-labeled neurons (Fig. 1). While Sstr3-positive cilia were not found on the other investigated cell types, colabeling also revealed the rare presence of AC3-positive cilia on GFAP-stained astrocytes (Bishop et al. 2007; Kasahara et al. 2014). Occurrence of Arl13b immunopositive cilia was strongly associated with GFAP positive astrocytes (Fig. 1). Although we also observed Arl13b positive primary cilia on neurons (Kasahara et al. 2014), the signal intensity of these cilia were faint and less apparent compared to the other two markers. Neither AC3 nor Arl13b immunoreactive cilia were observed on Iba-1-labeled microglia/macrophages or APC positive mature oligodendrocytes.

Comparative Distribution of Neuronal and Astrocytic Primary Cilia in the Mouse Brain

It has been previously reported that expression of certain ciliary markers are restricted to different regions of the brain (Bishop et al. 2007; Handel et al. 1999). To investigate whether there is a regional preference of primary cilia marker expression, we counted and compared the number of $AC3^+$/$NeuN^+$ and $Sstr3^+$/$NeuN^+$ neuronal primary cilia ($AC3^+$NPC and $Sstr3^+$NPC) as well as the $Arl13b^+$/$GFAP^+$ positive astrocytic primary cilia ($Arl13b^+$AsPC) of distinct areas of the brain. Our results were generally consistent with the earlier described data by others and were summarized in Supplementary Table (Online Resource, Table 1). We found that AC3, Sstr3, and Arl13b positive primary cilia were evenly distributed in the cingular, sensory, motor, and piriform cortices omitting the most superficial layer (Fig. 2). Among these regions both AC3 and Sstr3 showed the highest density in the piriform cortex where 53.73 and 29.68% of the cells had AC3- and Sstr3-positive cilia, respectively. The number of $Arl13b^+$AsPC was significantly less in all cortical regions (11.56–16.59%).

High number and a higher density of $AC3^+$NPC were found in the olfactory tubercule (91.8%), accumbens nucleus (85.36%), and caudo/putamen (81.3%), whereas a low number of $Arl13b^+$AsPC (8.2–18.69%) and no Sstr3 immunoreactive neuronal cilia were detected in these regions. In contrast, $Sstr3^+$NPC were observed in the claustrum and endopiriform nucleus (21.51 and 29.21%); however, their number was significantly lower compared to $AC3^+$NPC (61.49 and 63.66%).

In the hippocampus, both $AC3^+$NPC and $Sstr3^+$NPC were detected in all subregions of the stratum pyramidale. The number and density of Sstr3 followed a decreasing tendency, namely CA3 > CA2 > CA1, respectively. Notably, we observed a CA2 intersecting area where Sstr3 immunoreactivity only appeared in a punctate form surrounding the cell nuclei. The overall expression pattern of Sstr3 was found to be inversely proportionate to the number of $AC3^+$NPC. This trend was also observed in the dentate gyrus. In contrast to the neuronal ciliary markers, $Arl13b^+$AsPC showed an even distribution in the stratum oriens and radiatum bordering the pyramidal layer. Importantly, the density of $Arl13b^+$AsPC was the highest in the stratum lacunosum-moleculare and polymorph layer in the hippocampal formation.

We also found all three ciliary markers expressed in subnuclei of amygdala (Fig. 2). Although both $AC3^+$NPC and $Sstr3^+$NPC showed a higher density compared to $Arl13b^+$AsPC, the number of $AC3^+$NPC was significantly higher (61.67%) in contrast to $Sstr3^+$NPC (19.2%) or $Arl13b^+$AsPC (19.13%).

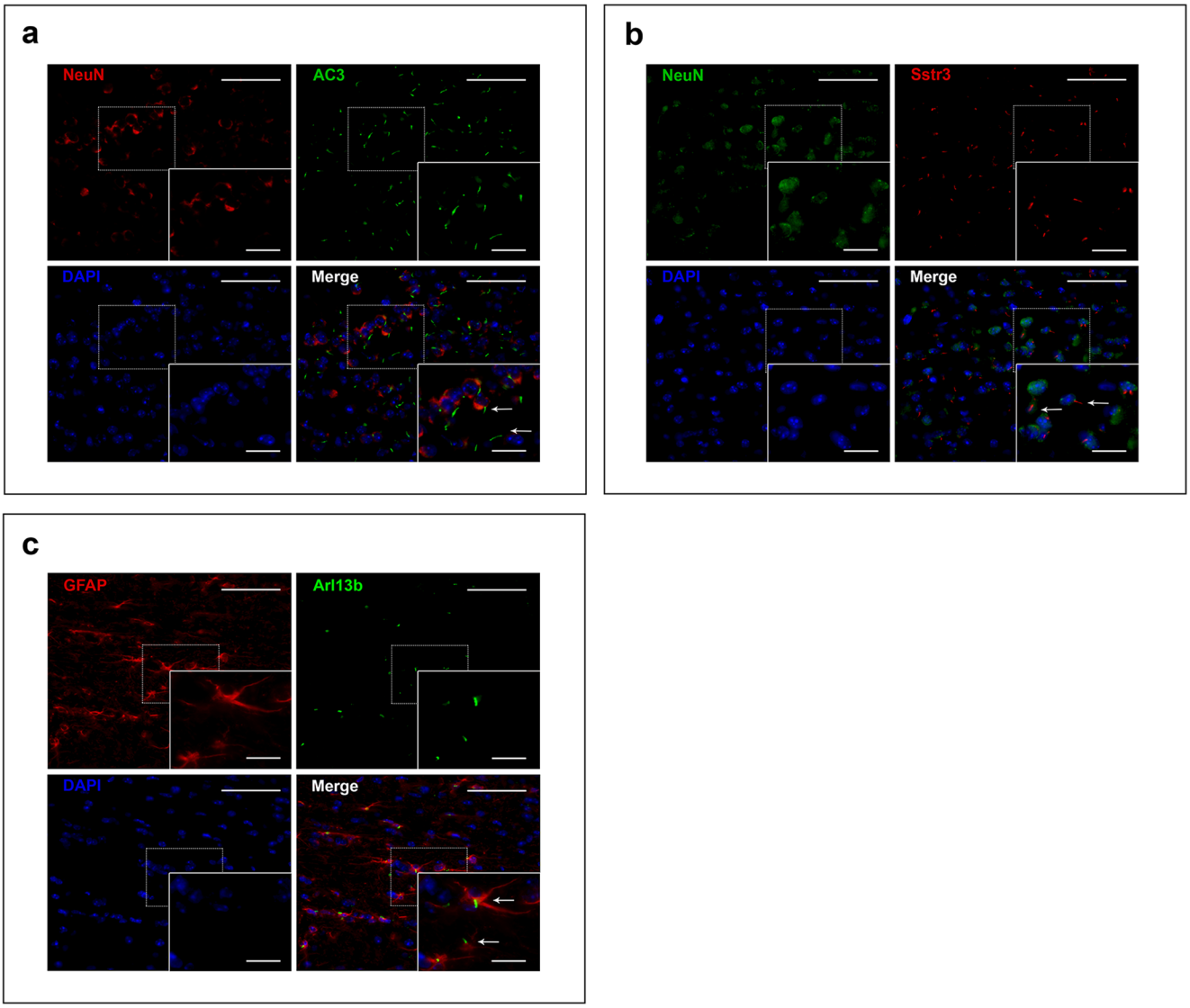

Fig. 1 Expression of primary cilia markers in the 8-week-old WT mouse brain. **a**, **b**, **c** Representative double fluorescent images of neurons and astrocytes colabeled for AC3, Sstr3, and Arl13b. **a**, **b** Primary cilia labeled with AC3 (green) and Sstr3 (red) localize to NeuN positive neurons (a—red and b—green). **c** Arl13b (green)-expressing primary cilia are associated with GFAP-positive astrocytes (red) as shown in corresponding overlays (scale bar 50 μm). Nuclei are visualized by DAPI (blue). The inserts in a, b, c panels indicate expression of the markers at higher magnification (scale bar 20 μm), and arrows show double labeled cells

In addition to the amygdala, the distribution and pattern of primary cilia also varied in the hypothalamic nuclei. Both $AC3^+$NPC and $Arl13b^+$AsPC were detected in all major subnuclei including the paraventricular (PVN), dorsomedial (DM), ventromedial (VM), arcuate (ARC), and suprachiasmatic (SCN) nucleus. The density and number of $AC3^+$NPC and $Arl13b^+$AsPC was the highest in the SCN (85.08%) and PVN (30.93%) regions, respectively. In contrast, ciliary expression of Sstr3 was limited to the VM in which 32.04% of the neurons had Sstr3-positive primary cilia. Although we did not find $Sstr3^+$NPC in the rest of the hypothalamic regions, we also observed a punctate Sstr3 immunoreactivity around cell nuclei similar to the hippocampal CA1-CA2 intersecting pattern (Fig. 2).

Regional Distribution of Primary Cilia Is Associated with Alterations of Their Length

Recent studies have demonstrated that ciliary signaling proteins can modulate primary cilia functions by dynamically regulating their length (Miyoshi et al. 2014; Parker et al. 2016). Based on the observed distributional patterns, to examine possible regional functions of primary cilia in the CNS, we measured and compared the length of neuronal and astrocytic primary cilia in the mouse brain.

We found that the average length of $AC3^+$NPC or $Sstr3^+$NPC was variable in the four investigated cortical regions within the range from 4.88 and 5.51 μm (cingular cortex) to 5.55 and 5.18 μm (piriform cortex), respectively.

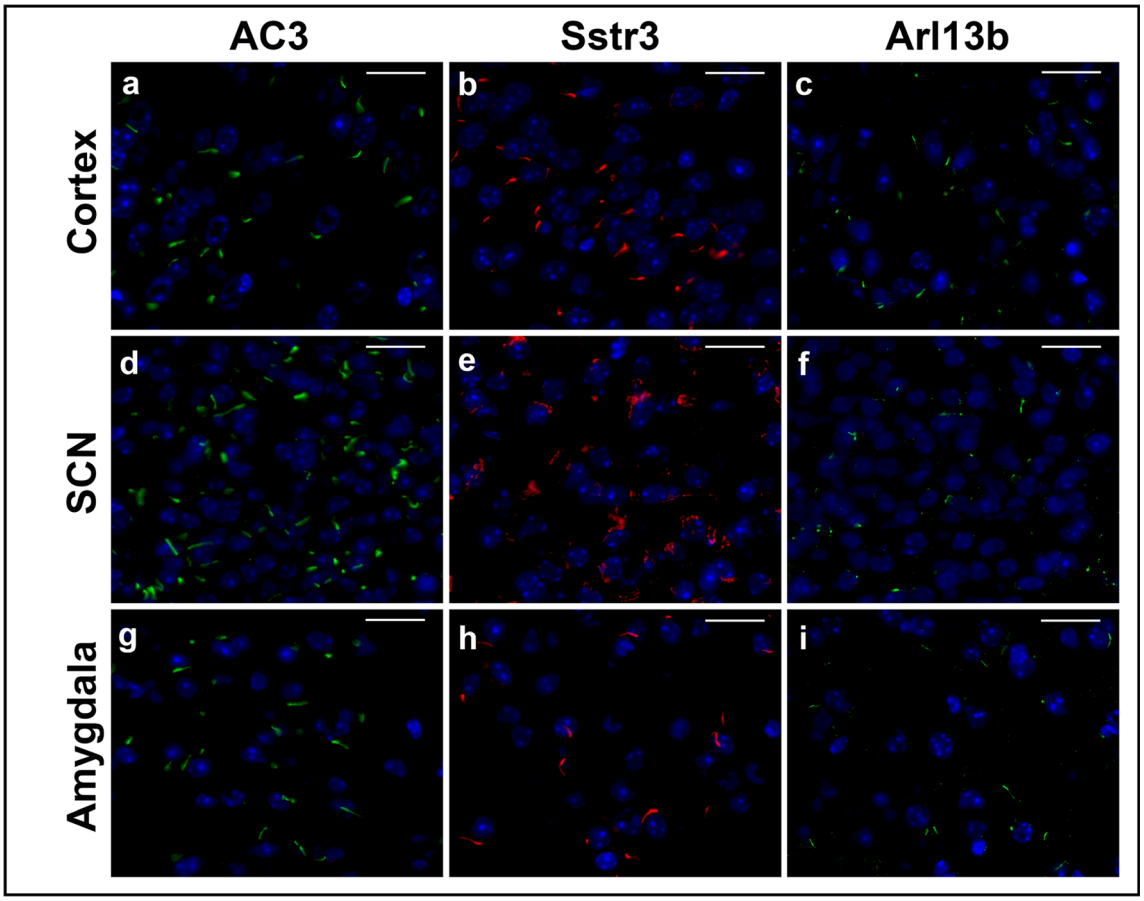

Fig. 2 Expression pattern and distribution of primary cilia markers in the mouse brain. **a**–**i** Representative fluorescent images of multiple brain regions showing primary cilia labeled for AC3 (green), Sstr3 (red), and Arl13b (green). **a**–**h** The number and density of AC3- and Sstr3-expressing primary cilia are inversely proportionate as shown in the cortical region (**a**, **b**), suprachiasmatic (**d**, **e**), and amygdaloid nucleus (**g**, **h**). Note that Sstr3 localizes to primary cilia in the cortical area (**b**) and amygdala (**h**), while Sstr3 immunoreactivity can only be seen in the cytoplasm in the suprachiasmatic nucleus (SCN) (**e**). The number of Arl13b-expressing primary cilia is less compared to AC3 or Sstr3, and only a few Arl13b-expressing cilia shows strong signal intensity (**c**, **f**, and **i**). Nuclei are stained with DAPI (blue). Scale bar 20 μm

Besides NPC, the average length of Arl13b$^+$AsPC varied between 2.95 and 3.33 μm. While Arl13b$^+$AsPC were significantly shorter compared to both types of NPC (***$P < 0.001$ and/or ****$P \leq 0.001$), comparison of AC3 and Sstr3$^+$NPC length did not reach a statistically significant value in either cortical region (Fig. 3).

Among the investigated brain regions, the average length of AC3$^+$NPC were measured essentially longer in the areas of the olfactory tubercule (10.68 μm), accumbens nucleus (9.84 μm) and caudo/putamen (9.61 μm) compared to the length of AC3$^+$NPC measured in the cortices. Additionally, the average length of both AC3 and Sstr3$^+$NPC were similarly short in the claustrum (5.41 and 4.92 μm) and endopiriform nucleus (6.16 and 5.14 μm) as in the cortical areas. Notably, AC3$^+$NPC were significantly longer compared to Sstr3$^+$NPC in the endopiriform region (***$P < 0.001$). Moreover, the average length of Arl13b$^+$AsPC ranged between 3.37–4.2 μm and was also significantly shorter compared to AC3$^+$NPC and/or Sstr3$^+$NPC in these areas (Fig. 3).

In the hippocampal CA regions, the average lengths of AC3$^+$NPC (5.0–5.91 μm) and Sstr3$^+$NPC (3.79–5.46 μm) showed a similar tendency to the cortices (Figs. 4 and 5). Importantly, AC3$^+$NPC (5.82 μm) were significantly longer compared to Sstr3$^+$NPC (3.79 μm) in the CA1 region (****$P \leq 0.001$). In addition, no significant differences were found comparing the average length of the AC3 and Sstr3$^+$NPC in the dentate gyrus (3.2 and 2.78 μm) and subnuclei of the amygdala (6.73 and 6.48 μm). The average length of Arl13b$^+$AsPC in the amygdala and hippocampus were identical to the cortical values (2.8–3.2 μm) and were significantly shorter in all of these regions but the area of the dentate gyrus.

We also found that AC3$^+$NPC were longer in the hypothalamus and its nuclei (Figs. 4 and 5). Their average length varied between 8.0 μm (PVN) and 10.48 μm (VM). Sstr3-expressing NPC were also detected longer in the VM (8.18 μm); however, these primary cilia appeared to be significantly shorter compared to AC3$^+$NPC in this region

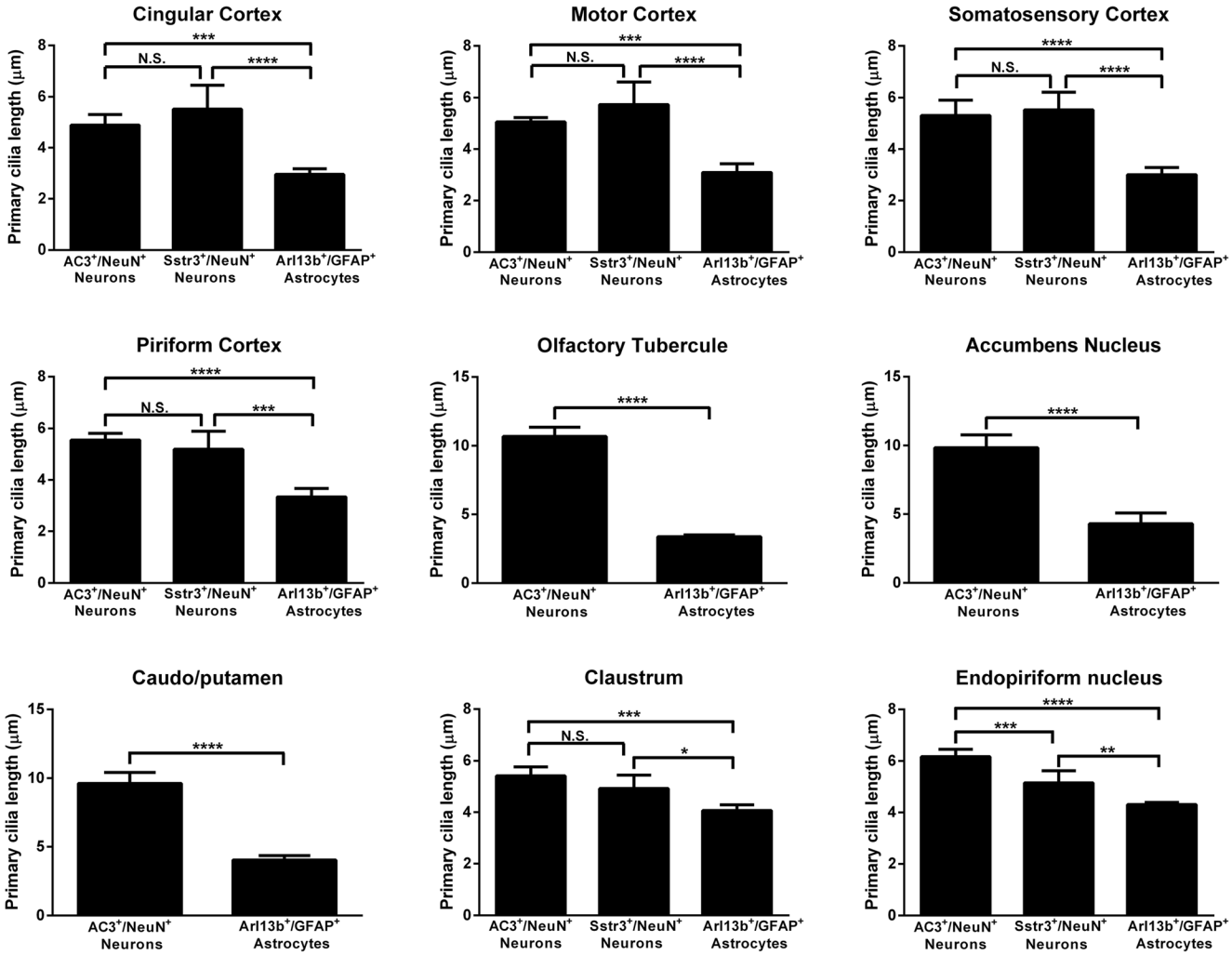

Fig. 3 Comparison of primary cilia length in the cortices, olfactory tubercule, caudo/putamen, claustrum, endopriform, and accumbens nucleus. Histograms show the length of $AC3^+/NeuN^+$, $Sstr3^+/NeuN^+$, and $Arl13b^+/GFAP^+$ double positive primary cilia measured ($n > 150$) from 5 animals per region. Columns represent the average length (mean ± SEM) of each primary cilia marker per brain region. Measurements were repeated three times and statistical differences were tested by Student's *t* test or one-way ANOVA followed by Tukey's multiple comparison post hoc test ($^*P < 0.05$, $^{**}P < 0.01$, $^{***}P < 0.001$, $^{****}P < 0.0001$) (GraphPad Prism software Version 6)

($^{**}P < 0.01$). Repeatedly, $Arl13b^+$AsPC were found significantly shorter (3.6–4.09 μm) in all nuclei of the hypothalamus ($^{****}P \leq 0.001$).

Discussion

Several previous studies have shown that primary cilia play a critical role in the development and maintenance of neural homeostasis of the mammalian brain (Fry et al. 2014; Lee and Gleeson 2010; Valente et al. 2014). Based on earlier observations (Bishop et al. 2007; Handel et al. 1999), possible functions of primary cilia can be specified by three major features: (1) the signaling molecules concentrated in the ciliary membrane, (2) the length of the structure, and (3) the cellular and regional localisation of the organelle within the CNS. Previous studies have elegantly mapped the distribution of AC3 and Sstr3-positive primary cilia in the brain (Bishop et al. 2007; Handel et al. 1999). In light of these fundamental reports, we intend to discuss our findings in connection with those and other studies underpinning a specific role of primary cilia in cell types and selected brain regions. Also, we aim to put emphasis on the regional traits and differences of ciliary marker expression that have not been described. One limitation of the present study is that accurate measurements of primary cilia length possess a technical challenge due to the 3D orientation and versatile expression of ciliary markers along the organelle's entire structural profile. However, currently, the main method of visualizing or quantifying primary cilia length on histological sections is still by immunofluorescence techniques utilizing cilia-specific antibodies. Therefore, we would like to

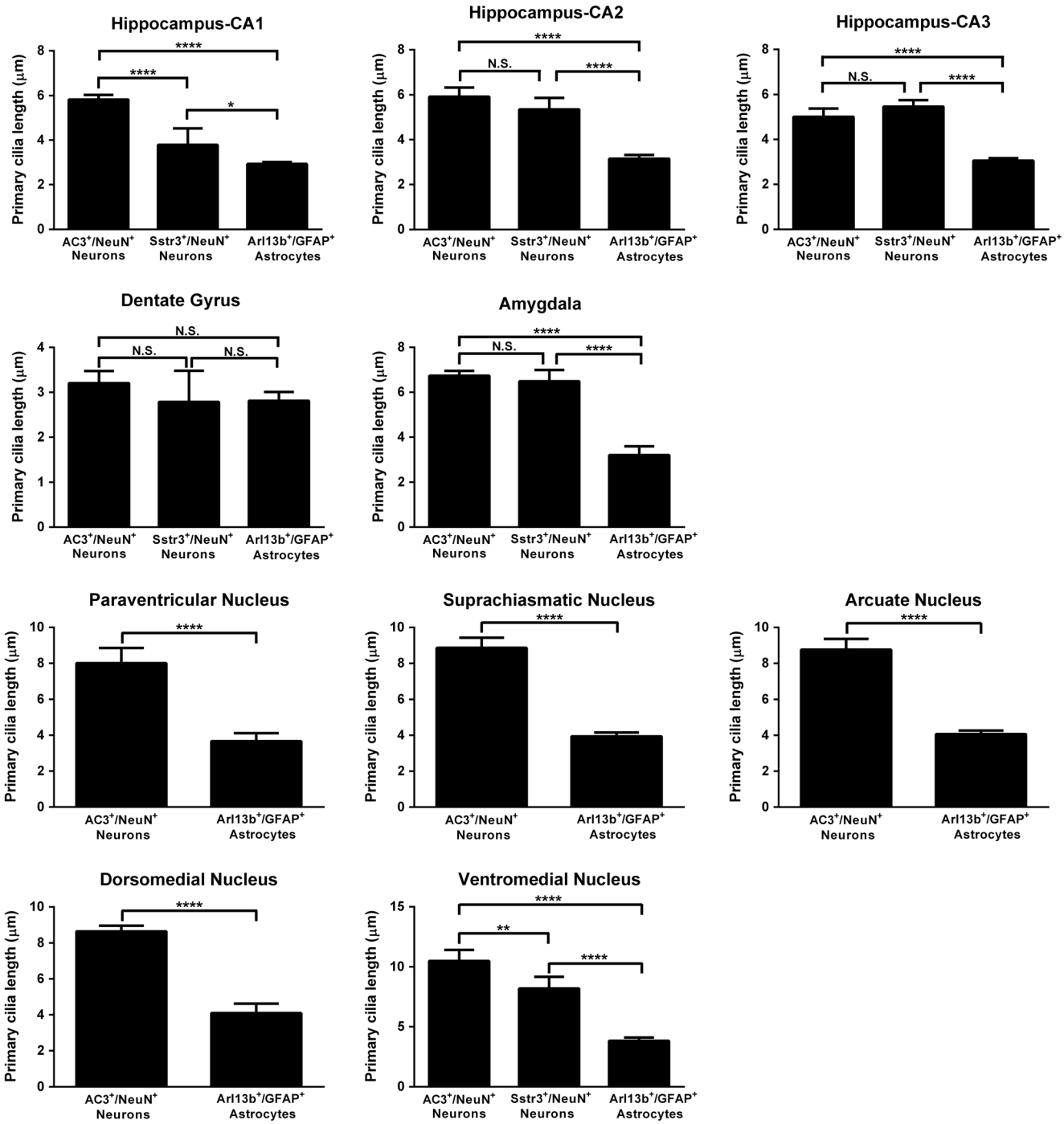

Fig. 4 Comparison of primary cilia length in the hippocampal formation and hypothalamic nuclei. Histograms show the length of $AC3^+/NeuN^+$, $Sstr3^+/NeuN^+$, and $Arl13b^+/GFAP^+$ double positive primary cilia measured ($n > 150$) from 5 animals per region. Columns represent the average length (mean ± SEM) of each primary cilia marker per brain region. Measurements were repeated three times, and statistical differences were tested by Student's *t* test or one-way ANOVA followed by Tukey's multiple comparison post hoc test (*$P < 0.05$, **$P < 0.01$, ****$P < 0.0001$) (GraphPad Prism software Version 6)

highlight the possibility that our findings might only reflect the immunohistochemically measurable length of primary cilia, and novel methods need to be developed to capture the true length of these organelles.

As the first step of our experiments, we characterized the expression of AC3-, Sstr3-, and Arl13b-positive primary cilia on different CNS cell types. In line with previous studies, we have confirmed that both AC3 and Sstr3 are predominantly

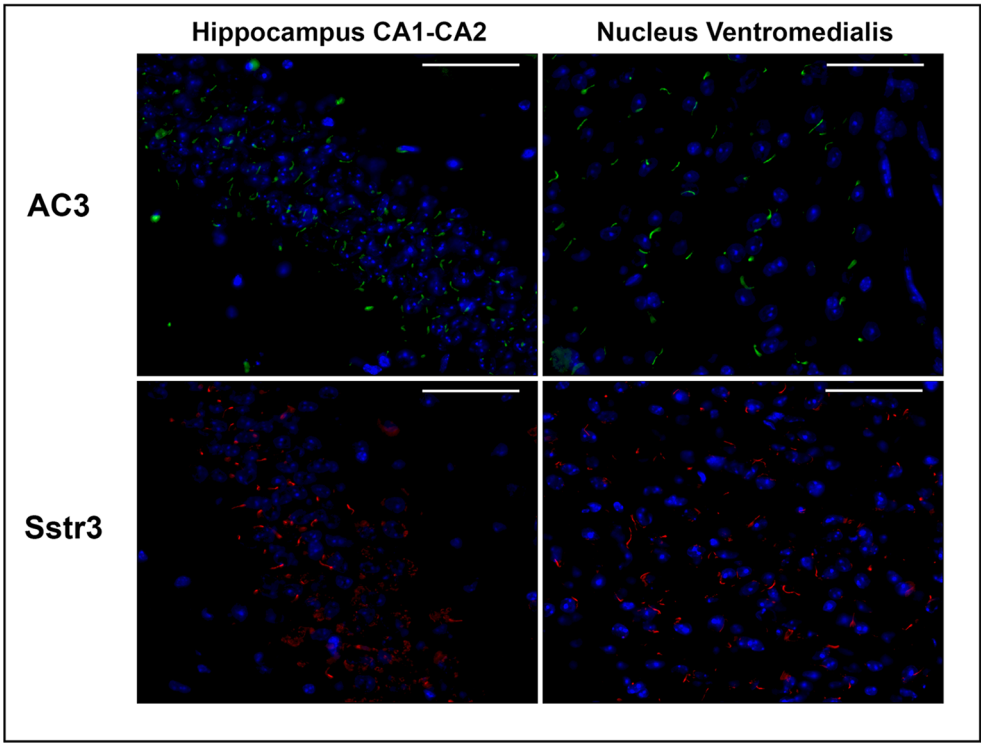

Fig. 5 Representative fluorescent images of the expression pattern and length of primary cilia labeled for AC3 and Sstr3 in the mouse brain. Labeling for AC3 (green) and Sstr3 (red) reveals numerous short primary cilia the hippocampus CA regions; however, Sstr3 immunoreactivity can also be seen in the cytoplasm. Note that the length of AC3 (green)- and Sstr3 (red)-positive cilia are longer in the ventromedial nucleus. Nuclei are visualized by DAPI (blue). Scale bar 50 μm

expressed on neuronal primary cilia (NPC) in the adult mouse brain. Although double immunolabeling revealed faint Arl13b-positive primary cilia on neurons, apparent Arl13b expression was associated with astrocytic primary cilia (AsPC). Additionally, only a few AC3 immunoreactive cilia localized to astrocytes and neither of the markers were observed together with mature oligodendrocytes or microglia/macrophages. The expression and frequency of Sstr3 positive NPC has been reported to change in parallel with the embryonic and postnatal development of the CNS (Stanic et al. 2009). Moreover, it has been demonstrated that AC3 as well as Arl13b expression of NPC and AsPC appear in a reciprocal manner in young aged (P10) compared to adult mice (P56) (Kasahara et al. 2014). Thus, our findings further indicate developmentally specified functions of primary cilia of CNS cell types, particularly on matured neurons and subpopulation of astrocytes.

To elucidate how neuronal or astrocytic primary cilia may influence brain functions, we examined and compared the expression pattern, length, and rate of occurrence of NPC and AsPC markers in regulatory centers of the CNS. In the present study, we confirmed that AC3 is the most abundant ciliary marker which can be detected throughout the brain, whereas Sstr3-positive cilia have a more restricted distribution. Additionally, the number and length of these NPC were variable and showed region-specific alternations. Notably, we found that $AC3^{+}$NPC were the densest and longest in the olfactory tubercule, supporting previous studies that implicated their significant role in olfaction (Challis et al. 2015; Kaupp 2010; Qiu et al. 2016; Wong et al. 2000). The length of $AC3^{+}$NPC were also measured longer in the caudo/putamen and accumbens nucleus. Since the protein components of primary cilia are thought to reflect distinct functional traits and we found ciliary morphology alike the olfactory tubercule, it is possible that the proper functioning of these regions may also substantially depend on AC3-linked pathways similar to odorant signaling. However, further studies are needed in this direction.

Expression pattern and length of AC3 were also comparable to Sstr3 immunoreactive neuronal cilia within the other investigated regions. Previous studies have demonstrated that $Sstr3^{+}$NPC are scarce in areas where AC3 expressing cilia are prevalent (Bishop et al. 2007). Indeed, we show that the number of $Sstr3^{+}$NPC is inversely proportionate to $AC3^{+}$NPC counted in regions, particularly in the cortices and hippocampus. As reported by others, our co-immunolabeling revealed two distinct expression profiles (Berbari et al. 2007; Berbari et al. 2008b; Green et al. 2016), indicating that only a certain population of neurons possesses Sstr3-positive cilia in both of these regions. Interestingly, we observed Sstr3 immunoreactive cell bodies in an intersecting area of the hippocampal pyramidal layer. The fact that AC3 localizes to cilia in this region and Sstr3 is retained in the cellular compartment indicates that ciliary localization of signaling proteins is strictly regulated and the precise functions of NPC may vary within neuronal subpopulations. It has been previously demonstrated that Sstr3-induced signaling is interconnected with adenylyl cyclase in the hippocampus (Einstein et al. 2010), and genetic

ablation of both AC3 and Sstr3 has a major impact on several region related functions such as forms of memory in mice (Chen et al. 2016; Einstein et al. 2010; Guadiana et al. 2013; Wang et al. 2011). Moreover, dynamic changes of ciliary protein expression and length have been also described in response to pharmacological or agonist treatment (Green et al. 2016; Parker et al. 2016). Thus, further studies are needed to examine whether primary cilia of those hippocampal neurons may transport receptors from the cells and consequently alter their length or influence neuronal function in the adult brain under different experimental conditions such as stress.

It is also important to note that the number and density of $Sstr3^{+}$NPC detected in the hippocampal dentate gyrus differs from a previous report (Stanic et al. 2009), where the density of Sstr3 immunoreactive cilia gradually increased by time and remained at high levels in the adult rat brain. A possible reason for this discrepancy may be due to the antibody and immunolabeling method applied in contrast to antisera that has been previously utilized. Indeed, similar procedure-related observations have been previously described (Hua and Ferland 2017). Another possibility is that our results may reflect age- and/or species-associated alternations between the brains of rodents.

Primary cilia have also been implicated in the hypothalamic control of appetite and feeding behaviour. Genetic modulation of ciliary expression can profoundly influence the regulation of food intake (Berbari et al. 2013; Davenport et al. 2007; Loktev and Jackson 2013; Mok et al. 2010; Mukhopadhyay and Jackson 2013; Qiu et al. 2016; Seo et al. 2009; Wang et al. 2009). Consistent with other work, we detected numerous AC3-positive neuronal primary cilia in all hypothalamic subnuclei, supporting that AC3 positive cilia are probably involved in the central regulation of appetite. In contrast to AC3, ciliary expression of Sstr3 was confined to the ventromedial nucleus and only cellular Sstr3 immunoreactivity was detected in the other hypothalamic nuclei. This distinct expression pattern of Sstr3 indicates that certain hypothalamic neuronal cilia might have multiple functional properties beyond the regulation of homeostatic functions. In particular, neuronal primary cilia have been demonstrated to express both Sstr3 and kisspeptin receptor 1 (kiss1r) on different population of hypothalamic neurons that are well-known central effectors driving the neuroendocrine axis such as growth hormone (GH) and gonadotropin-releasing hormone (GnRH) secretion (Brazeau et al. 1973; Johansson et al. 1984; Koemeter-Cox et al. 2014; Patel 1999; Yasuda et al. 1992). Moreover, recent immunhistochemichal study suggested that Sstr3 expressing primary cilia on GH secreting cells are necessary for sensing somatostatin in the adenohypophysis of mice (Iwanaga et al. 2011). In view of the literature along with our results, it is highly possible that Sstr3 positive cilia might mediate the biological effects of somatostatin on the neuroendocrine cells and within the local neural circuitry of the hypothalamus. It is also of note that both AC3- and Sstr3-positive cilia were measured the longest within the hypothalamic nuclei. Considering the complex nature of the hypothalamus, our data further indicate that enhanced ciliary length might be essential to sense multiple ligands and coordinate different signaling pathways in order to maintain region-specific functions. Indeed, it has been previously reported that cilia length on hypothalamic neurons are actively regulated according to different metabolic necessities and feeding state (Han et al. 2014). Therefore, longer ciliary length may also correlate with the ability to alter ligand binding sites and amplify the efficacy of signal transduction by transporting receptors from the neuronal plasma membrane. However, additional studies are required in the future to clarify this possibility.

The presence of astrocytic cilia had been previously described (Berbari et al. 2007; Bishop et al. 2007; Danilov et al. 2009; Doetsch et al. 1999); however, little is known about the physiological significance of primary cilia on these cell types. In the present study, we confirmed the majority of Arl13b-positive primary cilia localizes to astrocytes throughout the adult mouse brain, whereas only a few AC3 expressing cilia were detected on these cell types (Bishop et al. 2007; Kasahara et al. 2014). In view of the specific roles of astrocytes, this preferential expression indicates that there might be different populations of astrocytes, and Arl13b-signaling may provide an additional mechanism in regulating their region dependent functions. In particular, the number and density of Arl13b positive astrocytic cilia was higher in layers surrounding the hippocampal stratum granulare, a region important in generating new neurons from adult stem/progenitor cells. It has been demonstrated that primary cilia mediated Sonic Hedgehog (Shh) signaling is essential for the formation of hippocampal neural stem cells (Breunig et al. 2008; Han et al. 2008). Notably, conditional deletion of Arl13b disrupts critical cilium-mediated signaling pathways such as Shh (Caspary et al. 2007). Therefore, it is possible that Arl13b-signaling through the non-germinal astrocytes may contribute to a permissive environment to maintain neurogenesis in the dentate gyrus during perinatal as well as postnatal life. Another noteworthy observation is that astrocytic cilia were significantly shorter compared to neuronal cilia within all investigated brain regions. Additionally, quantitative comparison of their length also revealed differences between CNS regions; however, in some of the areas—linked average lengths of ARl13b-expressing cilia differ from those previously described (Kasahara et al. 2014). Considering all of our results, we presuppose the discrepancy may arise from the different labeling method and antibody applied similar to the variant expression pattern of Sstr3 positive cilia detected in the hippocampus. Arl13b belongs to the Ras GTPase superfamily and has well-established functions in diverse cellular processes. For example, primary cilia-mediated Arl13b signaling is required for

ciliary microtubule organization, ciliary membrane trafficking pathways, neuronal migration and formation of polarized radial glial scaffold in the developing nervous system (Caspary et al. 2007; Cevik et al. 2010; Higginbotham et al. 2012; Higginbotham et al. 2013; Humbert et al. 2012; Li et al. 2010). Signaling through AC3-positive astrocytic cilia have been suggested to provide and additional mechanism affecting synaptic transmission (Bishop et al. 2007). Therefore, it is intriguing to speculate a similar regulatory role influencing the biological functions of astrocytes. Nevertheless, the general presence and functional implications of Arl13b on astrocytic cilia is yet to be investigated in future experiments.

Conclusion

Primary cilia are tiny antenna-like cellular appendages that provide important sensory and signaling functions in the mammalian organ systems, particularly in the CNS. Although primary cilia are found to be widely distributed in the brain, the precise role of these organelles are just beginning to be understood. Importantly, studies of the last decade have highlighted that functions of neuronal cilia are reflected by the signaling molecules enriched in the ciliary membrane, their morphology, and localization in the CNS. In the present study, we aimed to quantify and compare the distribution and length of AC3-, Sstr3-, and Arl13b-expressing primary cilia in regions of the mouse brain. We show that primary cilia of neurons and astrocytes exhibit a well-defined range of ciliary marker expression. Moreover, the length, density, and occurrence rate of these markers display region-specific alternations, indicating various functions in the adult CNS. Collectively, our study provides a comprehensive overview of the regional and cellular organization of primary cilia in the physiological CNS, which serves an important tool in understanding the role of these organelles in future experiments.

Acknowledgements We thank Ms. Andrea Fábiánkovics and Ms. Krisztina Fülöp for their excellent technical assistance.

Funding Information The study was supported by a grant from the University of Pécs, Hungary (grant number: KA-2015-09).

Compliance with Ethical Standards

Animal experiments were conducted according to the European legislation on animal experimentation [Directives of the European Community (DIRECTIVE 2010/63/EU) and Hungarian regulations (40/2013, II.14)] in the laboratories of the University of Pécs.

The project was approved by local and national ethical boards and license was issued by government authorities (License No.:BA02/2000-44/2016 (KA-2068)).

References

Badano JL, Mitsuma N, Beales PL, Katsanis N (2006) The ciliopathies: an emerging class of human genetic disorders. Annu Rev Genomics Hum Genet 7(1):125–148. https://doi.org/10.1146/annurev.genom.7.080505.115610

Barker AR, Thomas R, Dawe HR (2014) Meckel-Gruber syndrome and the role of primary cilia in kidney, skeleton, and central nervous system development. Organ 10(1):96–107. https://doi.org/10.4161/org.27375

Berbari NF, Bishop GA, Askwith CC, Lewis JS, Mykytyn K (2007) Hippocampal neurons possess primary cilia in culture. J Neurosci Res 85(5):1095–1100. https://doi.org/10.1002/jnr.21209

Berbari NF, Johnson AD, Lewis JS, Askwith CC, Mykytyn K (2008a) Identification of ciliary localization sequences within the third intracellular loop of G protein-coupled receptors. Mol Biol Cell 19(4):1540–1547. https://doi.org/10.1091/mbc.E07-09-0942

Berbari NF, Lewis JS, Bishop GA, Askwith CC, Mykytyn K (2008b) Bardet-Biedl syndrome proteins are required for the localization of G protein-coupled receptors to primary cilia. Proc Natl Acad Sci U S A 105(11):4242–4246. https://doi.org/10.1073/pnas.0711027105

Berbari NF, Pasek RC, Malarkey EB, Yazdi SMZ, McNair AD, Lewis WR, Nagy TR, Kesterson RA, Yoder BK (2013) Leptin resistance is a secondary consequence of the obesity in ciliopathy mutant mice. Proc Natl Acad Sci U S A 110(19):7796–7801. https://doi.org/10.1073/pnas.1210192110

Bishop GA, Berbari NF, Lewis J, Mykytyn K (2007) Type III adenylyl cyclase localizes to primary cilia throughout the adult mouse brain. J Comp Neurol 505(5):562–571. https://doi.org/10.1002/cne.21510

Brailov I, Bancila M, Brisorgueil MJ, Miquel MC, Hamon M, Verge D (2000) Localization of 5-HT(6) receptors at the plasma membrane of neuronal cilia in the rat brain. Brain Res 872(1-2):271–275. https://doi.org/10.1016/S0006-8993(00)02519-1

Brazeau P, Vale W, Burgus R, Ling N, Butcher M, Rivier J, Guillemin R (1973) Hypothalamic polypeptide that inhibits the secretion of immunoreactive pituitary growth hormone. Science 179(4068):77–79. https://doi.org/10.1126/science.179.4068.77

Breunig JJ, Sarkisian MR, Arellano JI, Morozov YM, Ayoub AE, Sojitra S, Wang B, Flavell RA, Rakic P, Town T (2008) Primary cilia regulate hippocampal neurogenesis by mediating sonic hedgehog signaling. Proc Natl Acad Sci U S A 105(35):13127–13132. https://doi.org/10.1073/pnas.0804558105

Caspary T, Larkins CE, Anderson KV (2007) The graded response to Sonic Hedgehog depends on cilia architecture. Dev Cell 12(5):767–778. https://doi.org/10.1016/j.devcel.2007.03.004

Cevik S, Hori Y, Kaplan OI, Kida K, Toivenon T, Foley-Fisher C, Cottell D, Katada T, Kontani K, Blacque OE (2010) Joubert syndrome Arl13b functions at ciliary membranes and stabilizes protein transport in Caenorhabditis elegans. J Cell Biol 188(6):953–969. https://doi.org/10.1083/jcb.200908133

Challis RC, Tian H, Wang J, He J, Jiang J, Chen X, Yin W, Connelly T, Ma L, Yu CR, Pluznick JL, Storm DR, Huang L, Zhao K, Ma M (2015) An olfactory cilia pattern in the mammalian nose ensures high sensitivity to odors. Current biology : CB 25(19):2503–2512. https://doi.org/10.1016/j.cub.2015.07.065

Chen X, Luo J, Leng Y, Yang Y, Zweifel LS, Palmiter RD, Storm DR (2016) Ablation of type III adenylyl cyclase in mice causes reduced neuronal activity, altered sleep pattern, and depression-like phenotypes. Biol Psychiatry 80(11):836–848. https://doi.org/10.1016/j.biopsych.2015.12.012

D'Souza-Schorey C, Chavrier P (2006) ARF proteins: roles in membrane traffic and beyond. Nat Rev Mol Cell Biol 7(5):347–358. https://doi.org/10.1038/nrm1910

Danilov AI, Gomes-Leal W, Ahlenius H, Kokaia Z, Carlemalm E, Lindvall O (2009) Ultrastructural and antigenic properties of neural

stem cells and their progeny in adult rat subventricular zone. Glia 57(2):136–152. https://doi.org/10.1002/glia.20741

Davenport JR, Watts AJ, Roper VC, Croyle MJ, van Groen T, Wyss JM, Nagy TR, Kesterson RA, Yoder BK (2007) Disruption of intraflagellar transport in adult mice leads to obesity and slow-onset cystic kidney disease. Current biology : CB 17(18):1586–1594. https://doi.org/10.1016/j.cub.2007.08.034

Doetsch F, Garcia-Verdugo JM, Alvarez-Buylla A (1999) Regeneration of a germinal layer in the adult mammalian brain. Proc Natl Acad Sci U S A 96(20):11619–11624. https://doi.org/10.1073/pnas.96.20.11619

Domire JS, Green JA, Lee KG, Johnson AD, Askwith CC, Mykytyn K (2011) Dopamine receptor 1 localizes to neuronal cilia in a dynamic process that requires the Bardet-Biedl syndrome proteins. Cell Mol life Sci: CMLS 68:2951–2960. https://doi.org/10.1007/s00018-010-0603-4

Dummer A, Poelma C, DeRuiter MC, Goumans MJ, Hierck BP (2016) Measuring the primary cilium length: improved method for unbiased high-throughput analysis. Cilia 5(1):7. https://doi.org/10.1186/s13630-016-0028-2

Einstein EB, Patterson CA, Hon BJ, Regan KA, Reddi J, Melnikoff DE, Mateer MJ, Schulz S, Johnson BN, Tallent MK (2010) Somatostatin signaling in neuronal cilia is critical for object recognition memory. The Journal of neuroscience : the official journal of the Society for Neuroscience 30(12):4306–4314. https://doi.org/10.1523/JNEUROSCI.5295-09.2010

Forsythe E, Beales PL (2013) Bardet-Biedl syndrome. Eur J Hum Genet: EJHG 21(1):8–13. https://doi.org/10.1038/ejhg.2012.115

Franklin KBJ, Paxinos G (2008) The Mouse brain in stereotaxic coordinates. Elsevier Academic Press, Amsterdam

Fry AM, Leaper MJ, Bayliss R (2014) The primary cilium: guardian of organ development and homeostasis. Organ 10(1):62–68. https://doi.org/10.4161/org.28910

Gerdes JM, Davis EE, Katsanis N (2009) The vertebrate primary cilium in development, homeostasis, and disease. Cell 137(1):32–45. https://doi.org/10.1016/j.cell.2009.03.023

Gillingham AK, Munro S (2007) The small G proteins of the Arf family and their regulators. Annu Rev Cell Dev Biol 23(1):579–611. https://doi.org/10.1146/annurev.cellbio.23.090506.123209

Green JA, Schmid CL, Bley E, Monsma PC, Brown A, Bohn LM, Mykytyn K (2016) Recruitment of beta-arrestin into neuronal cilia modulates somatostatin receptor subtype 3 ciliary localization. Mol Cell Biol 36:223–235. https://doi.org/10.1128/MCB.00765-15

Guadiana SM, Semple-Rowland S, Daroszewski D, Madorsky I, Breunig JJ, Mykytyn K, Sarkisian MR (2013) Arborization of dendrites by developing neocortical neurons is dependent on primary cilia and type 3 adenylyl cyclase. The Journal of neuroscience : the official journal of the Society for Neuroscience 33(6):2626–2638. https://doi.org/10.1523/JNEUROSCI.2906-12.2013

Hamon M et al (1999) Antibodies and antisense oligonucleotide for probing the distribution and putative functions of central 5-HT6 receptors. Neuropsychopharmacology 21:68S–76S. https://doi.org/10.1016/S0893-133X(99)00044-5

Han YG, Spassky N, Romaguera-Ros M, Garcia-Verdugo JM, Aguilar A, Schneider-Maunoury S, Alvarez-Buylla A (2008) Hedgehog signaling and primary cilia are required for the formation of adult neural stem cells. Nat Neurosci 11(3):277–284. https://doi.org/10.1038/nn2059

Han YM, Kang GM, Byun K, Ko HW, Kim J, Shin MS, Kim HK, Gil SY, Yu JH, Lee B, Kim MS (2014) Leptin-promoted cilia assembly is critical for normal energy balance. J Clin Invest 124(5):2193–2197. https://doi.org/10.1172/JCI69395

Handel M et al (1999) Selective targeting of somatostatin receptor 3 to neuronal cilia. Neuroscience 89(3):909–926. https://doi.org/10.1016/S0306-4522(98)00354-6

Higginbotham H, Eom TY, Mariani LE, Bachleda A, Hirt J, Gukassyan V, Cusack CL, Lai C, Caspary T, Anton ES (2012) Arl13b in primary cilia regulates the migration and placement of interneurons in the developing cerebral cortex. Dev Cell 23(5):925–938. https://doi.org/10.1016/j.devcel.2012.09.019

Higginbotham H, Guo J, Yokota Y, Umberger NL, Su CY, Li J, Verma N, Hirt J, Ghukasyan V, Caspary T, Anton ES (2013) Arl13b-regulated cilia activities are essential for polarized radial glial scaffold formation. Nat Neurosci 16(8):1000–1007. https://doi.org/10.1038/nn.3451

Hilgendorf KI, Johnson CT, Jackson PK (2016) The primary cilium as a cellular receiver: organizing ciliary GPCR signaling. Curr Opin Cell Biol 39:84–92. https://doi.org/10.1016/j.ceb.2016.02.008

Hua K, Ferland RJ (2017) Fixation methods can differentially affect ciliary protein immunolabeling. Cilia 6(1):5. https://doi.org/10.1186/s13630-017-0045-9

Humbert MC, Weihbrecht K, Searby CC, Li Y, Pope RM, Sheffield VC, Seo S (2012) ARL13B, PDE6D, and CEP164 form a functional network for INPP5E ciliary targeting. Proc Natl Acad Sci U S A 109:19691–19696. https://doi.org/10.1073/pnas.1210916109

Iwanaga T, Miki T, Takahashi-Iwanaga H (2011) Restricted expression of somatostatin receptor 3 to primary cilia in the pancreatic islets and adenohypophysis of mice. Biomed Res 32(1):73–81. https://doi.org/10.2220/biomedres.32.73

Johansson O, Hokfelt T, Elde RP (1984) Immunohistochemical distribution of somatostatin-like immunoreactivity in the central nervous system of the adult rat. Neuroscience 13(2):265–339. https://doi.org/10.1016/0306-4522(84)90233-1

Kasahara K, Miyoshi K, Murakami S, Miyazaki I, Asanuma M (2014) Visualization of astrocytic primary cilia in the mouse brain by immunofluorescent analysis using the cilia marker Arl13b. Acta Med Okayama 68(6):317–322. https://doi.org/10.18926/AMO/53020

Kaupp UB (2010) Olfactory signalling in vertebrates and insects: differences and commonalities. Nat Rev Neurosci 11(3):188–200. https://doi.org/10.1038/nrn2789

Koemeter-Cox AI et al (2014) Primary cilia enhance kisspeptin receptor signaling on gonadotropin-releasing hormone neurons. Proc Natl Acad Sci U S A 111:10335–10340. https://doi.org/10.1073/pnas.1403286111

Larkins CE, Aviles GD, East MP, Kahn RA, Caspary T (2011) Arl13b regulates ciliogenesis and the dynamic localization of Shh signaling proteins. Mol Biol Cell 22(23):4694–4703. https://doi.org/10.1091/mbc.E10-12-0994

Lee JH, Gleeson JG (2010) The role of primary cilia in neuronal function. Neurobiol Dis 38(2):167–172. https://doi.org/10.1016/j.nbd.2009.12.022

Li Y, Wei Q, Zhang Y, Ling K, Hu J (2010) The small GTPases ARL-13 and ARL-3 coordinate intraflagellar transport and ciliogenesis. J Cell Biol 189(6):1039–1051. https://doi.org/10.1083/jcb.200912001

Loktev AV, Jackson PK (2013) Neuropeptide Y family receptors traffic via the Bardet-Biedl syndrome pathway to signal in neuronal primary cilia. Cell Rep 5(5):1316–1329. https://doi.org/10.1016/j.celrep.2013.11.011

Lu H, Toh MT, Narasimhan V, Thamilselvam SK, Choksi SP, Roy S (2015) A function for the Joubert syndrome protein Arl13b in ciliary membrane extension and ciliary length regulation. Dev Biol 397(2):225–236. https://doi.org/10.1016/j.ydbio.2014.11.009

Marshall JD, Maffei P, Collin GB, Naggert JK (2011) Alstrom syndrome: genetics and clinical overview. Current genomics 12(3):225–235. https://doi.org/10.2174/138920211795677912

Marshall WF, Nonaka S (2006) Cilia: tuning in to the cell's antenna. Current biology : CB 16(15):R604–R614. https://doi.org/10.1016/j.cub.2006.07.012

Miyoshi K, Kasahara K, Miyazaki I, Asanuma M (2009) Lithium treatment elongates primary cilia in the mouse brain and in cultured cells.

Biochem Biophys Res Commun 388(4):757–762. https://doi.org/10.1016/j.bbrc.2009.08.099

Miyoshi K, Kasahara K, Murakami S, Takeshima M, Kumamoto N, Sato A, Miyazaki I, Matsuzaki S, Sasaoka T, Katayama T, Asanuma M (2014) Lack of dopaminergic inputs elongates the primary cilia of striatal neurons. PLoS One 9(5):e97918. https://doi.org/10.1371/journal.pone.0097918

Mok CA, Heon E, Zhen M (2010) Ciliary dysfunction and obesity. Clin Genet 77(1):18–27. https://doi.org/10.1111/j.1399-0004.2009.01305.x

Mukhopadhyay S, Jackson PK (2013) Cilia, tubby mice, and obesity. Cilia 2(1):1. https://doi.org/10.1186/2046-2530-2-1

Ou Y, Ruan Y, Cheng M, Moser JJ, Rattner JB, van der Hoorn FA (2009) Adenylate cyclase regulates elongation of mammalian primary cilia. Exp Cell Res 315(16):2802–2817. https://doi.org/10.1016/j.yexcr.2009.06.028

Parisi MA (2009) Clinical and molecular features of Joubert syndrome and related disorders. Am J Med Genet C: Semin Med Genet 151C(4):326–340. https://doi.org/10.1002/ajmg.c.30229

Parker AK, le MM, Smith TS, Hoang-Minh LB, Atkinson EW, Ugartemendia G, Semple-Rowland S, Coleman JE, Sarkisian MR (2016) Neonatal seizures induced by pentylenetetrazol or kainic acid disrupt primary cilia growth on developing mouse cortical neurons. Exp Neurol 282:119–127. https://doi.org/10.1016/j.expneurol.2016.05.015

Patel YC (1999) Somatostatin and its receptor family. Front Neuroendocrinol 20(3):157–198. https://doi.org/10.1006/frne.1999.0183

Pissios P, Bradley RL, Maratos-Flier E (2006) Expanding the scales: the multiple roles of MCH in regulating energy balance and other biological functions. Endocr Rev 27(6):606–620. https://doi.org/10.1210/er.2006-0021

Qiu L, LeBel RP, Storm DR, Chen X (2016) Type 3 adenylyl cyclase: a key enzyme mediating the cAMP signaling in neuronal cilia. International journal of physiology, pathophysiology and pharmacology 8:95–108

Saghy E et al (2016) TRPA1 deficiency is protective in cuprizone-induced demyelination—a new target against oligodendrocyte apoptosis. Glia 64(12):2166–2180. https://doi.org/10.1002/glia.23051

Sattar S, Gleeson JG (2011) The ciliopathies in neuronal development: a clinical approach to investigation of Joubert syndrome and Joubert syndrome-related disorders. Dev Med Child Neurol 53(9):793–798. https://doi.org/10.1111/j.1469-8749.2011.04021.x

Schou KB, Pedersen LB, Christensen ST (2015) Ins and outs of GPCR signaling in primary cilia. EMBO Rep 16(9):1099–1113. https://doi.org/10.15252/embr.201540530

Seo S, Guo DF, Bugge K, Morgan DA, Rahmouni K, Sheffield VC (2009) Requirement of Bardet-Biedl syndrome proteins for leptin receptor signaling. Hum Mol Genet 18(7):1323–1331. https://doi.org/10.1093/hmg/ddp031

Singla V, Reiter JF (2006) The primary cilium as the cell's antenna: signaling at a sensory organelle. Science 313(5787):629–633. https://doi.org/10.1126/science.1124534

Stanic D, Malmgren H, He H, Scott L, Aperia A, Hokfelt T (2009) Developmental changes in frequency of the ciliary somatostatin receptor 3 protein. Brain Res 1249:101–112. https://doi.org/10.1016/j.brainres.2008.10.024

Valente EM, Rosti RO, Gibbs E, Gleeson JG (2014) Primary cilia in neurodevelopmental disorders. Nat Rev Neurol 10(1):27–36. https://doi.org/10.1038/nrneurol.2013.247

Wang Z, Li V, Chan GC, Phan T, Nudelman AS, Xia Z, Storm DR (2009) Adult type 3 adenylyl cyclase-deficient mice are obese. PLoS One 4(9):e6979. https://doi.org/10.1371/journal.pone.0006979

Wang Z, Phan T, Storm DR (2011) The type 3 adenylyl cyclase is required for novel object learning and extinction of contextual memory: role of cAMP signaling in primary cilia. The Journal of neuroscience : the official journal of the Society for Neuroscience 31(15):5557–5561. https://doi.org/10.1523/JNEUROSCI.6561-10.2011

Wong ST, Trinh K, Hacker B, Chan GCK, Lowe G, Gaggar A, Xia Z, Gold GH, Storm DR (2000) Disruption of the type III adenylyl cyclase gene leads to peripheral and behavioral anosmia in transgenic mice. Neuron 27(3):487–497. https://doi.org/10.1016/S0896-6273(00)00060-X

Yasuda K, Rens-Domiano S, Breder CD, Law SF, Saper CB, Reisine T, Bell GI (1992) Cloning of a novel somatostatin receptor, SSTR3, coupled to adenylylcyclase. J Biol Chem 267(28):20422–20428